Current-Induced Breakdown of Carbon Nanofiber Interconnects

Hirohiko Kitsuki, Tsutomu Saito, Toshishige Yamada, Drazen Fabris,
Patrick Wilhite, Makoto Suzuki, and Cary Y. Yang
Center for Nanostructures, Santa Clara University
Santa Clara, California 95053-0569, USA
Phone +1-408-554-6817, Fax: +1-408-554-5474, E-mail: kituki@mac.com

Abstract- **Current-induced breakdown phenomena of carbon nanofibers (CNFs) for future on-chip interconnect applications are presented. The effect of heat dissipation via the underlying substrate is studied using different experimental configurations. Scanning electron microscopy (SEM) techniques are utilized to study the structural damage by current stress. While the measured maximum current density in the suspended CNF in air is inversely proportional to nanofiber length and independent of diameter, SiO_2-supported CNFs improves their current capacity, which implies effective heat dissipation to the oxide. The correlation between maximum current density and electrical resistivity confirms the importance of local Joule heating, showing strong coupling between electrical and thermal transport in CNFs.**

I. Introduction

Copper interconnect is rapidly proceeding toward its minimization limit as a result of material failure due to electromigration. Carbon-based nanostructures such as carbon nanotubes (CNTs) [1-5] and carbon nanofibers (CNFs) [6,7] are being investigated for high-performance device and interconnect applications, because of their high electrical and thermal conductivities as well as current capacity. The growth of CNFs consistently yields high conductivity and high directionality, which are attractive for realistic interconnect fabrication processes [6]. In our previous study [7], CNF vias embedded in SiO_2 demonstrated high degree of reliability while being subjected to a stressing current of 1×10^7 A/cm^2. Thus such a structure is expected to achieve the current density target set by the International Technology Roadmap for Semiconductors (ITRS) [8] for the year 2015.

In CNT systems, breakdown phenomena have been observed under high electric fields, including nonlinear transport in single-walled CNTs [9] and successive graphitic wall breakdown in multi-walled CNTs [10]. In recent studies [7,11], proof of concept of the high-current reliability of CNFs for on-chip interconnects and the high-field transport properties of CNFs have been demonstrated. These results indicate that CNF breakdown mainly depends on resistive heating [12], but details of the failure mode due to high current and the accompanying physical breakdown mechanisms have yet to be investigated. While current annealing has been reported to drastically reduce the overall resistance and attributable to significant lowering of contact resistances in CNT devices [13][14], the significance of Joule heating in current-induced breakdown [11] implies that thermal contact coupling between CNF, electrodes, and surrounding materials (e.g., SiO_2) affects the current capacity of the CNF. In this work, the effect of heat dissipation via the electrodes and underlying substrate is studied for CNFs under high-current stress using different experimental configurations.

II. Experiment

The CNF samples are grown by plasma-enhanced chemical vapor deposition (PECVD) with a Ni catalyst layer on Si substrate. The detailed growth conditions have been described elsewhere [14]. Figure 1(a) shows a CNF sample suspended between gold electrodes, with a SEM image at 75° tilted-angle view. This planar geometry is a model of horizontal on-chip interconnect configuration, where the CNF sidewall is in contact with the electrodes [15]. A DC current source connected to these electrodes is also shown in Fig. 1(a). Constant-current stress (equivalent to current annealing) is then carried out to monitor the electrical resistance prior to breakdown in air. In order to study the failure mode of the CNFs fabricated in a more realistic device structure on a Si substrate, CNFs supported by SiO_2 are also examined, as shown in Fig. 1(b). Results for twenty devices, with CNFs ranging from 100 to 200 nm in diameter and 1.5 to 6 μm in length, are presented in this paper.

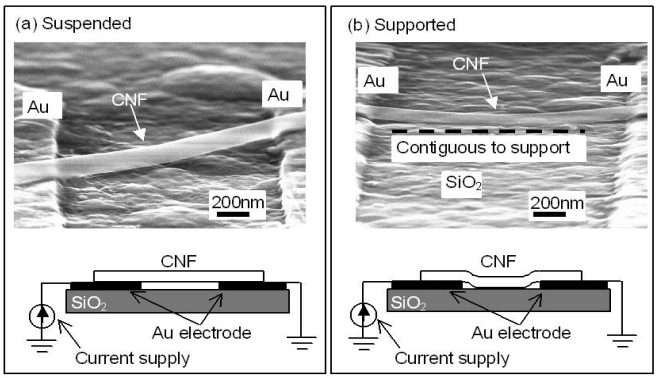

Fig. 1 Set-up for current-stressing experiments. (a) CNF suspended by gold electrodes. (b) CNF supported by SiO_2 substrate. Upper figures show SEM image of a CNF sample at 75° tilted-angle view, lower figures illustrate schematic of electrical measurement.

The progression of constant-current stress cycles (at 180 sec. each) is illustrated in Fig. 2(a). At the end of each cycle, *I-V* characteristics are obtained around $V = 0$. Figure 2(b) shows the resistance of a suspended CNF device after each annealing cycle versus annealing current. Increasing the annealing current

results in a gradual decrease in resistance before the nanofiber breaks down, at 700 μA for this particular device. The measured resistance consists of CNF bulk and contact resistance between the fiber and electrodes, and the CNF consistently breaks near the middle. This result implies that current annealing reduces the contact resistances significantly, while the device approaches breakdown due to resistive Joule heating in the bulk of the CNF.

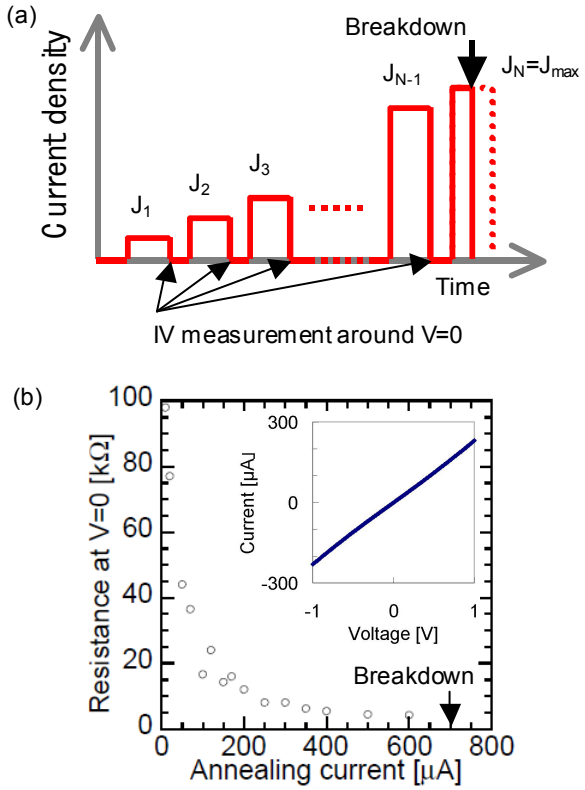

Fig.2 Resistance reduction of CNF device due to current annealing. (a) Schematic of successive current annealing cycles using stepwise increment of stressing current. (b) Resistance of the suspended CNF device at V=0 obtained after each annealing cycle. The inset shows the current-voltage behavior at the end of one of the anneal cycles.

III. Results and Discussion

SEM image of a CNF suspended by gold electrodes before and after current-induced breakdown is shown in Fig. 3(a). In all experiments for suspended CNFs, we have confirmed that breakdown always occurs near the middle of the nanofiber. This is consistent with diffusive heat transport observed in CNTs at high bias [10], suggesting that resistive heating [12] is critical to CNF breakdown.

For CNFs supported by SiO_2, result of current-induced breakdown is shown in Fig. 3(b). The interface between CNF and the substrate is imaged using SEM contrast [16]. A dark-contrast region along the CNF indicates a section of the nanofiber contiguous to the substrate, while the bright section is not in contact or suspended. Breakdown occurs in the segment where CNF is suspended above the substrate. It is expected that there is more heat transfer from CNF to substrate in the supported segment, thus resulting in higher current capacity than the suspended CNF. Meanwhile, the suspended segment is prone to failure because of poor thermal coupling to surrounding materials.

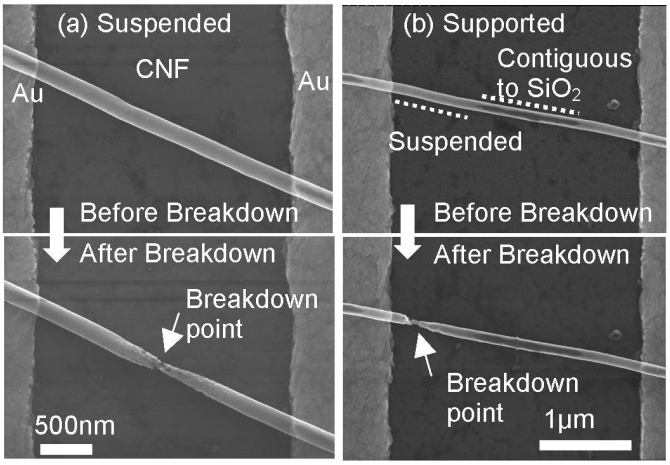

Fig. 3 SEM images of CNFs before and after current stressing at the top view. (a) CNF suspended by gold electrode. (b) CNF supported by SiO_2 substrate.

Figure 4 shows the relationship between the maximum current density (J_{max}) and reciprocal CNF length. Data obtained for the suspended CNF are given by solid circles. The decrease of J_{max} with increasing length is consistent with current-induced breakdown of single-walled carbon nanotubes (SWNT) [17] and gold nanowires fabricated using conventional lithography [18]. It should be noticed that a rapid current sweep of a few seconds led to breakdown near the electrodes, far from the middle of the fiber, suggesting substantial Joule heating due to contact resistance. Consequently, the measured J_{max} deviates significantly from the J_{max} versus length behavior as shown in Fig. 4. The entire annealing sequence as illustrated in Fig 2(b) typically takes about 45 minutes, consistently resulting in breakdown near the middle of the nanofiber as shown in Fig 3(a). The successive current annealing process effectively reduces the rise in temperature at or near the electrodes due to gradual decrease of contact resistance and more time for heat dissipation via the contacts, making the Joule heating along the CNF length the primary contribution to breakdown. This observed behavior is useful for predicting the current capacity of CNFs with different lengths when designing interconnects.

A one-dimensional thermal transport model [12,19] is used to analyze correlation between the observed current capacity J_{max} and length L of the CNFs, and the results is given by [20]

$$J_{\max} = \left[(T_{\max} - T_{\infty})\sigma\gamma w / A\right]^{1/2}\left[1 - 1/\cosh(aL/2)\right]^{-1/2}. \quad (1)$$

Here $a^2 = w\gamma/A\kappa$, where σ is the electrical conductivity, κ the CNF thermal conductivity, w the effective contact line width, and γ a coupling coefficient to account for the efficiency of heat transport through the CNF surroundings. T_{max} is the temperature at the breakdown point and T_∞ the ambient temperature. In the suspended case, heat

dissipation is expected to be negligible, or $aL << 1$. In this limit [20],

$$J_{\max} \approx 2\sqrt{2(T_{\max} - T_{\infty})\sigma\kappa} / L \qquad (2)$$

In Fig. 4, the measured $J_{\max}$ is plotted as a function of $1/L$. It is seen that the $J_{\max}$ versus $1/L$ behavior can be fitted to a straight line, as predicted by Eq. (2). For breakdown of SWNTs, a similar development using heat transport equation yielded the same result as here [9]. This agreement confirms that for a suspended CNF, heat dissipation to the surroundings (air) is small, and heat conduction along the length of the CNF causes the highest temperature to occur at the middle of CNF.

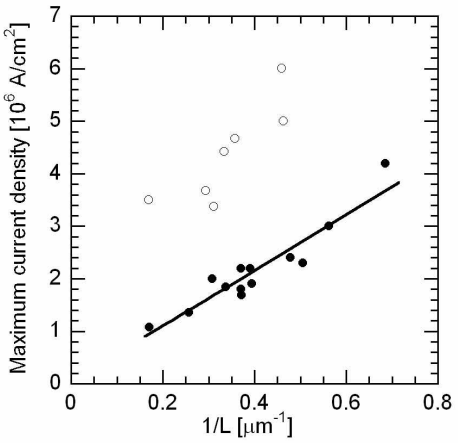

Fig. 4 Dependence of maximum current density on CNF length obtained using 20 devices. The solid and open circles show the results for suspended and supported CNFs, respectively. The straight line is a linear fit for suspended CNFs, as predicted by the heat transport model.

The maximum current density observed for the supported configuration is plotted with open circles in Fig. 4. The supported CNFs show significantly improved current capacity in comparison to the suspended CNFs. However, the dependency of maximum current density on length is not as clear. While J_{max} increases with with decrease in CNF length as in the suspended case, its behavior is largely affected by the area in contact with the support material, which contributes significantly to the heat dissipation process. This finding indicates that heat dissipation via its immediate surroundings is a critical determining factor for high-current transport in CNF. While the contrast in SEM images is useful to estimate where the CNF is contiguous to the supporting SiO_2, thermal coupling between the nanofiber and the substrate is yet to be investigated for analyzing the current capacity versus the length behavior.

Combining the experimentally fitted line for $J_{\max}$ versus $1/L$ in Fig. 4 with Eq. (2), $T_{\max} = 1260$ K for the suspended CNFs. Here, a CNF thermal conductivity of 12 W/m K [21] is used for the calculation of critical temperature. While the thermal contact resistance was reduced by platinum coating on the CNFs [21], the breakdown near the middle of the fiber as shown in Fig. 3(a) seems to suggest that successive current annealing improves thermal conductivity as well. Regarding σ, we use the maximum electrical conductivity prior to the breakdown from the present data. Despite of the CNFs grown using the same process, the measured conductivity varies within a factor of two after the annealing process. For MWNTs under high current stress, the conductivity drastically decreases due to successive graphitic wall removal [10]. In addition, current-voltage characteristics of CNTs saturate in the high-current region, being attributed to electron-phonon scattering [22,23]. Meanwhile, the resistance of CNF is monotonically reduced during the annealing steps as shown in Fig 2(b). It can be assumed that, the improvement in conductance is dominated by changing the coupling between CNFs and the electrodes, and significant contact resistance still remains even in late annealing cycles, resulting in variation of the measured conductivity. Thus the maximum conductivity obtained with two-point current stress measurements can be assumed to approach the CNF conductivity.

This result for $T_{\max} = 1260$ K is comparable to the CNF synthesis temperature, estimated to be in the 1000 K range [24]. For current-induced breakdown of CNTs, critical temperature under high current stress has been experimentally obtained as above 800 K [9,25]. Though having no radiative heat transfer and in the limit of no coupling with the substrate, the temperature obtained is only an indication of CNF durability, it is a reasonable estimation of critical temperature for CNF breakdown and points to the need for systematic local temperature measurement.

IV. Conclusion

We have investigated experimentally the CNF breakdown caused by high-current stress using two distinct geometrical configurations. With reduced contact resistance due to current annealing, it is found that the maximum current density monotonically decreases with increasing CNF length for both suspended and supported fibers. In the suspended case, a simple heat transport model confirms the observed linear J_{max} versus $1/L$ behavior. The effective heat dissipation by the surrounding materials and ambient is shown to improve the nanofiber's current-carrying capacity, and the present study represents an important first step toward the understanding of the reliability of CNF for potential interconnect applications.

Acknowledgment

The authors are grateful to John R. Jameson of Santa Clara University, Jun Li of Kansas State University, and Alan M. Cassell of NASA Ames Research Center for their helpful advice. They also thank Hitachi High-technologies America for its assistance in electron microscopy. This work was supported by the United States Army Space and Missile Defense Command (SMDC) and carries Distribution Statement A, approved for public release, distribution unlimited.

REFERENCES

[1] See, e.g., "*Carbon Nanotubes: Synthesis, Structure, Properties, and Applications,*" ed. by M. S. Dresselhaus, G. Dresselhaus, and Ph. Avouris, Boston:, Springer, 2001.

[2] R. Martel, T. Schmidt, H.R. Shea, T. Hertel, P. Avouris, "*Single- and multi-wall carbon nanotube field-effect transistors* ," *Appl. Phys. Let*t. Vol. 73, pp. 2447-2449, October 1998

[3] A. Javey, J. Guo, Q. Wang, M. Lundstrom, H. Dai, "*Ballistic carbon nanotube field-effect transistors*," *Nature*, Vol. 424, pp. 654-657, August 2003.

[4] T. Yamada, "*Modeling of carbon nanotube Schottky barrier modulation under oxidizing conditions*," *Phys. Rev*. B, Vol. 69, 125408, June 2004.

[5] M. Nihei, M. Horibe, A. Kawabata, Y. Awano, "*Simultaneous Formation of Multiwall Carbon Nanotubes and their End-Bonded Ohmic Contacts to Ti Electrodes for Future ULSI Interconnects*," *Japan. J. Appl. Phys*., Vol. 43, pp. 1856-1859, April 2004.

[6] J. Li, Q. Ye, A.M. Cassell, H.T. Ng, R. Stevens, J. Han, M. Meyyappan, "*Bottom-up approach for carbon nanotube interconnects*," *Appl. Phys. Lett*., Vol. 82, pp. 2491-2493, April 2003.

[7] Q. Ngo, A.M. Cassell, A.J. Austin, J. Li, S. Krishnan, M. Meyyappan, C.Y. Yang, "*Characteristics of aligned carbon nanofibers for interconnect via applications*," *IEEE Electron Device Lett*., Vol. 27, pp. 221-224, April 2006.

[8] International Technology Roadmap for Semiconductors (ITRS) 2006 Update. [Online]. Available: http://public.itrs.net

[9] E. Pop, D.A. Mann, J. Cao, K.E. Goodson, H. Dai, "*Electrical and thermal transport in metallic single-wall carbon nanotubes on insulating substrates*," *J. Appl. Phys*., Vol. 101, 093710, May 2007.

[10] J.Y. Huang, S. Chen, S.H. Jo, Z. Wang, D.X. Han, G. Chen, M.S. Dresselhaus, Z.F. Ren, "*Atomic-scale imaging of wall-by-wall breakdown and concurrent transport measurements in multiwall carbon nanotubes*," *Phys. Rev. Lett*., Vol. 94, 236802, June 2005.

[11] M. Suzuki, Y. Ominami, Q. Ngo, C.Y. Yang, J. Li, A.M. Cassell, "*Current-induced breakdown of carbon nanofibers*," *J. Appl. Phys*., Vol. 101, 114307, June 2007.

[12] M.A. Kuroda, A. Cangellaris, J.-P. Leburton, "*Nonlinear transport and heat dissipation in Metallic carbon nanotubes*," *Phys. Rev. Lett*., Vol. 95, 266803, December 2005.

[13] J.-O Lee, C. Park, J.-J. Kim, J. Kim, J.W. Park, K.-H. Yoo, "*Formation of low-resistance ohmic contacts between carbon nanotube and metal electrodes by a rapid thermal annealing method*," *J. Phys. D*., Vol. 33, pp. 1953-1956, August 2000.

[14] B.A. Cruden, A.M. Cassell, Q. Ye, M. Meyyappan, "*Reactor design considerations in the hot filament/direct current plasma synthesis of carbon nanofibers,*" *J. Appl. Phys*., Vol. 94, pp. 4070-4078, June 2003.

[15] L. Zhang, D. Austin, V.I. Merkulov, A.V. Meleshko, K.L. Klein, M.A. Guillorn, D.H. Lowndes, M.L. Simpson, "*Four-probe charge transport measurements on individual vertically aligned carbon nanofibers*," *Appl. Phys. Lett*. Vol. 84, pp. 3972-3974, May 2004.

[16] M. Suzuki, Y. Ominami, Q. Ngo, C.Y. Yang, T. Yamada, J. Li, A.M. Cassell, "*Bright contrast imaging of carbon nanofiber-substrate interface*," *J. Appl. Phys*., 100, 104305, November 2006.

[17] E. Pop, D. Mann, J. Cao, Q. Wang, K. Goodson, H. Dai, "*Negative Differential Conductance and Hot Phonons in Suspended Nanotube Molecular Wires*," *Phys. Rev. Lett*., Vol. 95, 155505, October 2005.

[18] C. Durkan, M.A. Schneider, M.E. Welland, "*Analysis of failuar mechanisms in electrically stressed Au nanowires*," *J. Appl. Phys*., Vol. 86, pp. 1280-1286, April 1999.

[19] H.S. Carslaw, J.C. Jaeger, *Conduction of Heat in Solids Second Edition*; Oxford University Press, Oxford, 1986.

[20] H. Kitsuki, T. Yamada, D. Fabris, J.R. Jameson, P.Wilhite, M. Suzuki, C.Y Yang, "*Length dependence of current-induced breakdown in carbon nanofiber interconnects*," *Appl. Phys. Lett*., Vol. 92, 173110, May 2008.

[21] C. Yu, S. Saha, J. Zhou, L. Shi, A.M. Cassell, B.A. Cruden, Q. Ngo, J. Li., "*Thermal Contact Resistance and Thermal Conductivity of a Carbon Nanofiber*," *J. Heat Transfer*, Vol. 128, pp. 234-239, March 2006

[22] Z. Yao, C. L. Kane, and C. Dekker, "*High-Field Electrical Transport in Single-Wall Carbon Nanotubes*," *Phys. Rev. Lett*. Vol. 84, pp. 2941-2944, March 2000.

[23] P.G. Collins, M. Hersam, M. Arnold, R. Martel, P. Avouris, "*Current Saturation and Electrical Breakdown in Multiwalled Carbon Nanotubes*," *Phys. Rev. Lett*., Vol. 86, pp. 3128-3131, April 2001.

[24] K.B.K. Teo, D.B. Hash, R.G. Lacerda, N.L. Rupesinghe, M.S. Bell, S.H. Dalal, D. Bose, T.R. Govindan, B.A. Cruden, M. Chhowalla, G.A.J. Amaratunga, M. Meyyappan, W.I. Milne, "*The Significance of Plasma Heating in Carbon Nanotube and Nanofiber Growth*," *Nano Lett*., Vol. 4, pp. 921-926, April 2004.

[25] T. D. Yuzvinsky, W. Mickelson, S. Aloni, S. L. Konsek, A. M. Fennimore, G. E. Begtrup, A. Kis, B. C. Regan, and A. Zettl., "*Imaging the life story of nanotube devices*," *Appl. Phys. Lett*. Vol. 87, 083103, August 2005.